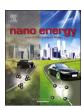


Contents lists available at ScienceDirect

Nano Energy

journal homepage: www.elsevier.com/locate/nanoen



Full paper

Ligand engineering on CdTe quantum dots in perovskite solar cells for suppressed hysteresis



Jia-Wen Xiao^{a,1}, Sai Ma^{a,1}, Shijie Yu^a, Chenxiao Zhou^a, Pengfei Liu^a, Yihua Chen^b, Huanping Zhou^b, Yujing Li^{a,*}, Qi Chen^{a,*}

- ^a Beijing Key Laboratory of Nanophotonics and Ultrafine Optoelectronic Systems, School of Materials Science and Engineering, Beijing Institute of Technology, Beijing 100081, PR China
- Department of Materials Science and Engineering, College of Engineering, Peking University, Beijing 100871, PR China

ARTICLE INFO

Keywords: Perovskite solar cells CdTe Quantum dots Ligand exchange Hysteresis

ABSTRACT

Solar cells employing lead halide perovskites as light absorbers have been one hot topic in recent years due to their amazing device performance and commercialization potential. Yet, there exist challenges on the way to their practical use, including long-term stability, and J-V hysteresis. Herein, we demonstrate an improved contact between perovskite and hole transporting layer (HTL) by using CdTe quantum dots, wherein the capping ligands on quantum dots are systematically investigated. The devices with the CdTe quantum-dot-in-perovskite solids interlayer achieve a high efficiency (~ 19.3%, averaged), and more importantly, a significantly reduced hysteresis, which is superior to devices with CdTe QDs capped by other ligands (PbI₂, CH₃NH₃I, oleic acid). We attribute this superior device performance to the congeneric junction contact between perovskite and CdTe quantum-dot-in-perovskite layer. Furthermore, we reveal that the reduced hysteresis is partially contributed from faster hole extraction at the interface thanks to the high hole mobility in CdTe. These findings shed lights on the future design of quantum dots for perovskite optoelectronics in the perspective of ligand engineering.

1. Introduction

Perovskite (PVSK) solar cells have attracted tremendous attention due to its rapidly growing power conversion efficiencies (PCEs) and low fabrication cost [1–3]. The PCEs of PVSK photovoltaics skyrocketed from 3.9% in 2009 to over 22% in 2016 [4,5]. And it is believed that the PCEs can be further improved through compositional engineering, materials design, and interface engineering, etc [6]. Although substantial success has been achieved for PVSK solar cells, serious challenges impede its practical applications, such as the long-term stability, large-scale fabrication, and J-V hysteresis [7,8]. The notorious J-V hysteresis is particularly pronounced in planar p-i-n structured PVSK solar cells, which hinders the accurate characterization of their photovoltaic performance [9].

Interface engineering represents one effective approach to further improve the device performance and alleviate the J-V hysteresis since interfaces in PVSK solar cells play vital roles in charge carrier transportation, extraction, and collection [10–12]. Various materials and/or methods have been reported to modify the interfaces between PVSK and hole transporting layer (HTL) or electron transporting layer (ETL), such as fullerene and their derivative [13], CsBr [14], amino acid [15], and inorganic quantum dots

[16-20], etc. Among all these modifiers, inorganic quantum dots (QDs) show their tunability by taking advantages of their size- and surface-dependent optoelectronic properties. For instance, graphene QDs incorporated between TiO2 ETL and PVSK layer were shown to enhance the device efficiency due to the improved electron extraction [16]. PbS QDs were used as an inorganic HTL in PVSK solar cells to harvest the infrared solar light [21]. However, there lacks of systematic investigation to reveal how the surfaces of these QDs affects device performance, wherein surface passivation of QDs leads to efficient photovoltaic devices [22-24]. In particular, these interface modification methods introduce two new heterojunction interfaces in devices upon the addition of QDs, congeneric materials with similar crystal structure and composition employed in the interfaces would be preferable for charge carrier transport and extraction. For example, Wang et al. used MAPbBr3-xIx QDs as an interface modifier between MAPbI3 and HTL to enhance the interfacial charge transfer [17], the MAPbBr_{3-x}I_x QDs is congeneric with MAPbI₃.

In this paper, we focused on improving the hole extraction efficiency between PVSK and HTL to enhance the PCEs and alleviate J-V hysteresis. Previous studies found that holes tended to accumulate at the hole transport layer of Spiro-OMeTAD, which resulted in unbalanced charge transport

^{*} Corresponding authors.

E-mail addresses: yjli@bit.edu.cn (Y. Li), qic@bit.edu.cn (Q. Chen).

¹ Contributed equally to this work

J.-W. Xiao et al. Nano Energy 46 (2018) 45–53

[25]. Introducing an interlayer with high hole mobility between PVSK and Spiro-OMeTAD provides a feasible solution. CdTe is a direct-bandgap, ptype semiconductor, which show high hole mobility [26]. However, to take advantage of the high mobility of CdTe to achieve high performance PVSK solar cells, the surface passivation of CdTe QDs and the band alignment between PVSK and CdTe should be carefully examined. Herein, we incorporated CdTe quantum-dot-in-perovskite solids at PVSK/HTL interface to construct congeneric junction contact between the absorber and HTL, leading to PVSK solar cells with high efficiency and suppressed hysteresis. CdTe QDs with suitable bandgap were first synthesized, and followed by ligand exchange to produce the CdTe-QD-in-perovskite solids (CdTe-MAPbI₃). Due to the high hole mobility of CdTe and the good energy alignment between PVSK and HTL, the CdTe-MAPbI3 interlayer allowed fast hole extraction from PVSK to HTL, which significantly reduced the device hysteresis. Moreover, the CdTe-MAPbI3 interlayer was proposed to reduce the carrier recombination in PVSK layer and PVSK-HTL heterojunction. Our results provide a facile strategy to alleviate the notorious hysteresis issue in PVSK solar cells.

2. Results and discussions

2.1. Synthesis and ligand exchange of CdTe QDs

The CdTe quantum dots (QDs) were synthesized through the classical hot-injection method and cleaned by the solvent/anti-solvent method [27] (see experimental section for details). Briefly, a Cd precursor was made by dissolving 10 mmol of CdO in oleic acid (OA) and 1-octadecene (ODE) under N_2 atmosphere. Meanwhile, a Te precursor was prepared by dissolving certain amount of Te powder in tri-n-butylphosphine (TBP) and ODE. Then, the Te precursor was swiftly injected into the Cd precursor solution at 300 °C. The obtained QDs were cleaned by ethanol and toluene for several times before further use. Transmission electron microscopy (TEM) characterization (Fig. 1a and b) showed that the as-synthesized CdTe QDs displayed an irregular multi-pods morphology, along with some spherical dots. The high-resolution TEM (HRTEM) in Fig. 1c shows the lattice fringe of CdTe QDs, and the lattice fringe spacings of 0.22 nm and 0.37 nm correspond to the (110) and (002) plane of the wurtzite CdTe, respectively.

The oleate capping group on the QDs rendered them a good dispersity in non-polar solvent such as hexane, as shown in Fig. 1(a). However, these long-chain ligands would impede the carrier transport on QD surface when they are incorporated in optoelectronic devices, which leads to poor device performance. Therefore, we performed a ligand exchange procedure to remove the long-chain oleate group. The ligand exchange procedure was conducted according to Yang's method [28], by which a thin PVSK shell was formed on the QDs. Briefly, a certain amount of CdTe-QD-dispersed-hexane solution was mixed with the dimethyl formamide (DMF) dissolved with perovskite precursor (0.3 M CH₃NH₃I and PbI₂). After vigorous stirring for ~ 5 min, the CdTe QDs were transferred into the polar DMF phase, indicating the successful ligand exchange. After washing and precipitation, a mixed solvent containing n-butylamine and toluene (4/1 in volume) was used to disperse the CdTe QDs, after which the ligand-exchanged QDs can re-disperse in non-polar solvent such as chlorobenzene. We speculate that nbutylamine (BA) molecules would help to switch the solubility of ligandexchanged QDs from polar solvent to non-polar solvent through the interaction between amine group and the surface PVSK on CdTe QDs [29]. Thus, the ligand-exchanged CdTe QDs dispersed in chlorobenzene can be deposited atop the PVSK layer without affecting its film quality, since polar solvent such as DMF, BA would destroy the PVSK film by solvation. On the other side, the non-polar solvent also facilitates the formation of PVSK on CdTe surface. Fig. 1d and e showed that the CdTe QDs after ligand exchange turned out to form a network-like structure. We proposed that CdTe-QD-inperovskite solids were formed, which was also reported by other group using the similar ligand exchange method [30-33]. The HRTEM image in Fig. 1f showed a lattice fringe spacing of 0.32 nm, which corresponds to the (004) lattice plane of MAPbI₃ [34]. It is worth to note that the organicinorganic hybrid $MAPbI_3$ is sensitive to strong electron beam, the electron beam damage should be taken into consideration when carrying out HRTEM characterization [35]. So we tried to decrease the electron beam dose rate and shorten the exposure time during the TEM characterization. The details were shown in the experimental section. The scheme in Fig. 1g showed the whole ligand exchange process of CdTe QDs.

After the ligand exchange, the CdTe QDs maintained its hexagonal crystal structure confirmed by X-ray powder diffraction (XRD) as shown in Fig. 2a. It is found that a new peak appeared around 27.8° (20). We ascribed this peak to the diffraction of (004) lattice plane of tetragonal MAPbI₃ [34]. Other XRD peaks of MAPbI₃ cannot observed due to the low crystallinity and the strong background peak, UV-Vis absorption spectroscopy in Fig. 2b demonstrated that the exciton absorption peak of CdTe ODs located around 700 nm. From the absorption spectrum and Tauc plot, we estimated the bandgap of CdTe QDs to be 1.74 eV. Due to the quantum confinement effect, CdTe QDs show a size-dependent bandgap behavior. With decreasing size of QDs, the valence band maximum (VBM) will gradually decrease, while the conduction band minimum (CBM) would gradually increase [36]. According to the VBM and CBM of hybrid perovskite and Spiro-OMeTAD [37], it is better if the VBM of CdTe QDs locate in $-5.4 \,\mathrm{eV} \sim -5.2 \,\mathrm{eV}$ (relative to vacuum energy level). Considering the bandgap (1.5 eV) and VBM of bulk CdTe 1.5 eV[38], the bandgap of CdTe QDs should be around 1.7 \sim 1.9 eV. CdTe QDs with too large bandgap or too small bandgap would result in unfavored energy alignment when they are incorporated between hybrid perovskite and Spiro-OMeTAD, which is detrimental to the solar cell performance. Thus, the bandgap of our synthesized CdTe QDs matches well with the interface energetics of PVSK solar cells. The exact VBM and CBM of CdTe QDs were measured by ultraviolet photoelectron spectroscopy (UPS), which will be discussed later.

To further confirm the formation of MAPbI $_3$ perovskite around CdTe QDs, the element mapping was conducted by energy dispersive X-ray spectroscopy (EDX) in STEM, as shown in Fig. S1. The mapping results clearly showed that both Pb and I can be detected around the CdTe QDs aggregation, and N can also be observed, which confirmed the formation of CdTe-QD-inperovskite solids. The X-ray photoelectron spectroscopy (XPS) results of CdTe QDs before and after ligand exchange were demonstrated in Fig. S2. We found that an additional peak at high binding energy appeared in the Te 3d core-level spectra after ligand exchange, this peak was attributed to the high valence state (+4) of Te [39], which means that a certain amount of Te²⁻ was oxidized to Te⁴⁺ by oxygen during the ligand exchange process. Both of the Pb 4 f and N 1 s core-level signal can be found in CdTe-QD-in-perovskite solids, and the spectra were similar to that of MAPbI $_3$ film, which also corroborates the formation of PVSK after the ligand exchange process.

To confirm the successful ligand-exchange, the Fourier transfer infrared spectroscopy (FT-IR) was used to examine the surface organic species on QDs. As shown in FT-IR (Fig. S3), the absorption peak around 1526 cm⁻¹ and 1407 cm⁻¹ in CdTe QDs resulted from the asymmetric and symmetric stretching vibration mode of carboxylate group of oleate [40,41]. However, these two peaks cannot be observed in CdTe QDs after ligand exchange, indicating that the majority of oleate group capping on CdTe QDs have been removed. After ligand exchange, the excitonic absorption peak of CdTe QDs disappeared (Fig. S4), which may be induced by the aggregation of QDs [42,43].

2.2. Device performance

To illustrate how the surface of CdTe QDs affects device performance, we introduced the CdTe QDs with different ligands as a modification layer between the PVSK and HTL in a systematic manner. The device architecture was illustrated in Fig. 3a. The device architecture adopted a conventional ni-p planar structure ITO/SnO₂/PVSK/CdTe-QD/Spiro-OMeTAD/Ag. To verify whether the band alignment of the incorporated CdTe-MAPbI₃ matches well with PVSK, the UPS measurement of CdTe-MAPbI₃ was conducted (Fig. S5). The VBM of CdTe-MAPbI₃ was extracted by using the log scale [37,44,45]. The result showed that the VBM of CdTe-MAPbI₃ was -5.3 eV, which was close to the VBM of PVSK (-5.4 eV). Considering that the

Download English Version:

https://daneshyari.com/en/article/7952776

Download Persian Version:

https://daneshyari.com/article/7952776

<u>Daneshyari.com</u>